PROCEEDINGS OF SCIENCE

Spectral and temporal properties of long GRBs detected by INTEGRAL from 3 keV to 8 MeV

A. Martin-Carrillo[*1], **M. Topinka**[1], **L. Hanlon**[1], **S. Meehan**[1], **S. Foley**[1,2], **B. McBreen**[1], **S. Brandt**[3], **D. Tierney**[1]

[1] *UCD School of Physics, Dublin, Ireland*
[2] *Max Planck Institut Garching (MPE)*
[3] *DTU, Denmark*
E-mail: antonio.martin-carrillo@ucd.ie

Since its launch in 2002, *INTEGRAL* has triggered on more than 78 γ–ray bursts in the 20-200 keV energy range with the IBIS/ISGRI instrument. Almost 30% of these bursts occurred within the fully coded field of view of the JEM-X detector (5°) which operates in the 3-35 keV energy range. A detailed study of the spectral and temporal evolution of a subset of 7 *INTEGRAL* γ–ray bursts across a wide energy range from 3 keV to 8 MeV has been carried out. This GRB sample is characterised by long multi-peaked bursts that are bright in the JEM-X energy range and encompass X-ray rich bursts, X-ray flashes and classical GRBs. We report the detection of X-ray prompt and afterglow emission from GRB 041219A and GRB 081003A with JEM-X for the first time. At least two temporal breaks have been identified in the X-ray afterglow light curve of GRB 081003A. These results demonstrate *INTEGRAL's* broadband capabilities for the study of the transition from X-ray prompt to afterglow emission in γ–ray bursts.

8th INTEGRAL Workshop "The Restless Gamma-ray Universe"- Integral2010,
September 27-30, 2010
Dublin Ireland

[*] Speaker.

PoS(INTEGRAL 2010)043

1. Introduction

Since its launch in October 2002 *INTEGRAL* [1] has triggered on more than 78 γ–ray bursts (GRBs) within the IBIS field of view (FOV) [2] (20-200 keV energy range), a rate of $\sim$0.8 GRBs/month. The triggering is done by the *INTEGRAL* Burst Alert System (IBAS)[1] [3], an automatic ground-based system providing a localisation accuracy of ~ 3 arcminutes. Due to the high sensitivity of the IBIS/ISGRI detector layer, *INTEGRAL* is one of the best observatories for the detection of faint GRBs (peak flux $\sim$0.1 ph cm^{-2} s^{-1}) [4]. In addition, *INTEGRAL* has broadband spectral capability afforded by IBIS ($9^\circ \times 9^\circ$ fully coded field of view), JEM-X (3–35 keV), with its $5^\circ \times 5^\circ$ fully coded field of view [5] and the SPI Germanium detector (20 keV to 8 MeV, $16^\circ \times 16^\circ$ fully coded field of view [6].

INTEGRAL's broad energy range provides a window to explore the emission processes which give rise to the GRB spectral characteristics. Despite the significant progress that has been made in the past decade in our understanding of the progenitors, afterglows, host galaxies and distances of GRBs, fundamental characteristics of the bursts themselves still remain unexplained. For example, it is not yet established how the observed non-thermal spectrum is produced despite major theoretical efforts [7]. The spectral output peaks at a few hundred keV and continues as a $\sim$ -2.2 power-law, consistent with the index expected from Fermi acceleration, extending up to GeV energies in some cases.

In the classical optically thin synchrotron shock model the γ–ray emission comes from an isotropic population of shock-accelerated electrons that have a power-law energy distribution above a characteristic cut-off energy. The spectra predicted by this model are asymptotically broken power-laws which are very reminiscent of the Band model (Band et al. 1993). However, in many cases the low-energy photon number index violates the -2/3 limit predicted in the simplest realisation of synchrotron emission [8]. Modified synchrotron models, incorporating features such as synchrotron cooling and/or an anisotropic distribution of electrons with small mean pitch angles can reproduce the global distributions of spectral parameters, but not all aspects of the observations. Taking these characteristics into account, along with new observations by *Fermi*/LAT of additional power-law components extending well into the GeV range [15], it is clear that the emission process is much more complex than 'straightforward' synchrotron radiation.

Further motivation for broadband GRB spectroscopy comes from observations by *BATSE* of a spectral excess between 5 and 10 keV in $\sim$ 14% of GRBs [9, 10], indicating the presence of an additional, possibly thermal, component to the synchrotron model. There is also evidence for a thermal component in the first stages of GRB emission which accompanies the underlying non-thermal emission [13, 12, 14] and which provides a natural explanation for the known correlation between peak energy and luminosity, since, for a thermal emitter, the luminosity and temperature are correlated. The thermal component may be attributable to photospheric emission, while the non-thermal component (spectral index varying from -1.5 to -2.1) at late times in the burst is consistent with the high-energy power-law of the synchrotron cooling spectrum. The thermal emission component has been shown to be a powerful new diagnostic tool for determining the initial size and Lorentz factor of GRB fireballs in a more model-independent way than other techniques [11] and requires broadband observations. The instruments on-board the *INTEGRAL* and *Fermi* observatories are

[1] `http://ibas.iasf-milano.inaf.it/IBAS_Results.html`

capable of studying simultaneous prompt emission in both the γ–ray and low X-ray (< 10 keV) energy bands.

The launch of *Swift* in 2004 represented a new era for the study of early time X-ray afterglows. For GRBs with prompt emission lasting ~ 100 s, *Swift* has been able to observe the transition phase between the final stages of the prompt emission and the beginning of the X-ray afterglow [16]. A dip feature has been observed in the X-ray hardness ratios of GRBs at the end of the steep decay phase [17], which can be interpreted as the turn on of the X-ray afterglow in accordance with previous predictions [18]. The JEM-X data can be used to independently verify the presence of the dip in the hardness ratio seen in some *Swift* bursts.

2. Data Sample and Analysis

Twenty one GRBs detected by IBIS/ISGRI have occurred within the 5° FOV of JEM-X to date. Most of these bursts were faint, with peak fluxes ≤ 0.7 ph cm^{-2} s^{-1} in the 20-200 keV energy range. All 21 bursts were detected by JEM-X with peak fluxes (3-35 keV) ranging between 1 and 39 ph cm^{-2} s^{-1}. A limit on the fluence (3-35 keV) of $\geq 2.5 \times 10^{-7}$ erg cm^{-2} was applied in this analysis to restrict the sample to bursts with sufficient statistics for spectroscopy. The final sample of 7 GRBs covers all three classes of GRBs based on their fluence ratios [19] i.e. classical GRBs, X-ray rich (XRR) bursts and X-ray flashes (XRF). The properties of the bursts in the sample are presented in Table 1.

The data from the three high energy instruments on board *INTEGRAL* were reduced using an automatic tool for GRB analysis (*grb_analyser*) built over the Off-line Science Analysis, OSAv9[2]. This tool also provides all the temporal properties of the bursts and, by an iterative procedure, the best response matrix for each burst. The data from each instrument were then combined for broadband spectral analysis using *XSPECv12.5*. The normalisations of the fits to the JEM-X and SPI data were allowed to float as free parameters in the joint spectral analysis. The calibrated normalisation factors provided by the ISDC team[3] (with IBIS/ISGRI as 1.0) are 0.95 for JEM-X and 1.19 for SPI. Due to the low statistics in the SPI detector for these events, the normalisation factor obtained was 1.5 ± 0.4, slightly greater than the calibrated value. Good agreement was found between the ISDC normalisation factor and the observed value for JEM-X (0.9 ± 0.4).

3. Results

The broadband spectrum of each GRB is fit with four spectral models: power-law, Band model, blackbody plus power-law and power-law with exponential cut-off. A summary of the GRB properties and best fit spectral results is given in Table 1 and some of the highlight results are presented in more detail below.

[2] http://www.isdc.unige.ch/integral/analysis#Documentation

[3] http://isdcul3.unige.ch/Soft/download/osa/osa_doc/osa_doc-9.0/osa_cross_cal-1.0.pdf

Table 1: Summary of properties and best fit spectral results for the 7 GRBs considered in the combined (JEM-X, IBIS and SPI) spectral analysis.'PF' is the peak flux in the 20-200 keV energy range; 'PL' is the power-law model, 'Band' is the Band model and 'BB+PL' is the blackbody plus power-law model. α and β represent the power-law indexes below and above the break energy.

GRBs	Class	T_{90} (sec)	PF (20-200 keV) ph cm^{-2} s^{-1}	Best fit	α	β	kT (keV)	E_{peak} (keV)	Red. χ^2/dof
040812	XRF	21	0.5	PL	—	-2.33±0.85	—	—	0.6/66
041219A	GRB	365	30	Band	-1.44±0.01	-2.06±0.05	—	146±11	1.54/212
050520	GRB	54	0.98	BB+PL	-1.49±0.09	—	22±4	—	0.68/76
051105B	XRR	13	0.31	PL	-1.91±0.06	—	—	—	0.63/49
080613	GRB	20	1.3	PL	-1.23±0.6	—	—	—	0.34/37
081003A	XRR	22	0.36	BB+PL	-1.66±0.11	—	6.4±0.8	—	0.77/44
081016	GRB	26	3.87	BB+PL	-1.66±0.09	—	18.6±1.7	—	0.88/56

3.1 GRB 041219A

Due to the extreme brightness of this GRB [12], there are substantial gaps in the IBIS/ISGRI data for most of the burst duration (Fig. 1, left panel). The 3-35 keV GRB lightcurve as seen by JEM-X is shown in Fig. 1 (right panel). The hardness ratio (Fig. 1, lower left) between the IBIS/ISGRI soft band (20-50 keV) and its hard band (50-200 keV) shows the typical hard to soft evolution with additional hardening at the onset of each pulse. Hardness-intensity tracking is also seen in the main pulses at T_0+300 s and T_0+385 s. A soft flare after the precursor, beginning at T_0+100 s (Fig. 1, right panel) is easily seen in the JEM-X lightcurve and is also observed below 50 keV by IBIS/ISGRI. The overall decline in the hardness ratio between the precursor and the flare indicates a possible connection between them. The increased hardness at the beginning of the major pulse at T_0+250 s, suggests that this is a separate flaring episode after a 100 s quiescent phase.

Due to the IBIS/ISGRI data gaps, only JEM-X and SPI are used for the broadband spectral analysis of the whole burst. As shown in Table 1, the reduced χ^2 for the best fit is significantly greater than 1, most probably due to the significant spectral variability during the burst (Fig. 1). However, the burst is sufficiently bright that the spectrum may also have been affected by instrumental systematics. Although the Band model is statistically a slightly better fit than the BB+PL model, the high energy tail seen in the multi-instrument time integrated spectrum is better fit by the BB+PL model.

3.2 GRB 081016

GRB 081016 was triggered by IBIS/ISGRI [20] as two bright pulses separated by less than 20 s (Fig. 2, left panel). The two pulses have almost equal amplitude between 50 and 200 keV, with the second pulse becoming more pronounced towards lower energies, indicative of significant softening. The first pulse is not detected below 10 keV.

The broadband multi-instrument spectrum over the T_{90} interval is shown in Fig. 2 (right panel). The best fit model (Table 1) shows a black-body component (kT=18.6±1.7 keV) with a high energy power-law tail.

3.3 X-ray afterglow emission

A search for X-ray (3-35 keV) afterglow emission (where burst duration is defined by the T_{90}

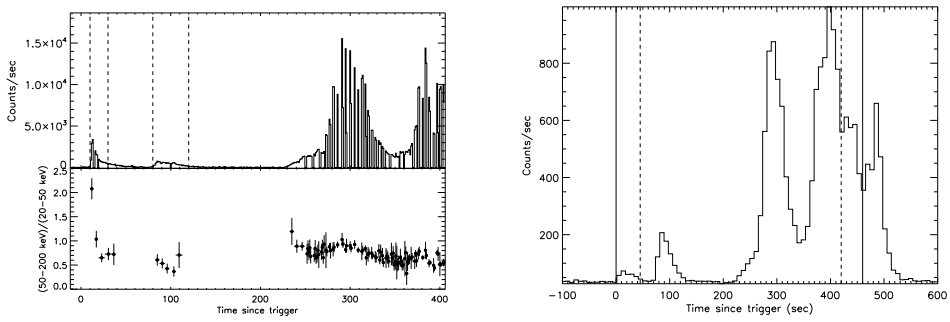

Figure 1: *Left:* GRB 041219A IBIS/ISGRI light curve in the 20-200 keV energy range. Data gaps in the brightest part of the GRB are caused by saturation of the detector. The standard analysis cuts the data at T_0+400 s although the pointing direction did not change until T_0+550 s. The dashed vertical lines show the 'precursor' and the 'soft flare' regions. *Right:* JEM-X lightcurve of GRB 041219A in the 3-35 keV energy range. The last 150 s of JEM-X data were recovered from the housekeeping data. The total and T_{90} durations measured in the γ-ray band are represented by the solid and dashed lines respectively.

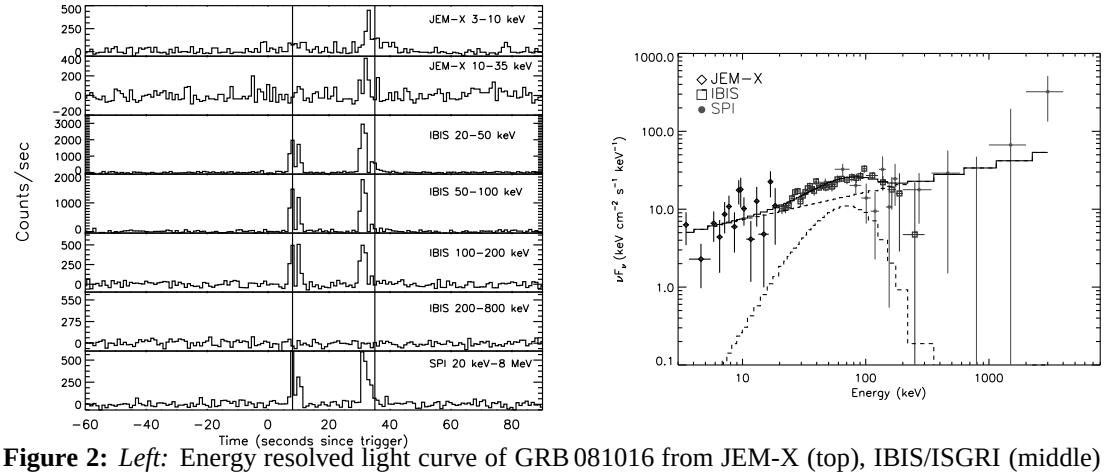

Figure 2: *Left:* Energy resolved light curve of GRB 081016 from JEM-X (top), IBIS/ISGRI (middle) and SPI (bottom). *Right:* The broadband spectrum of GRB 081016 from 3 keV to 4 MeV using data from JEM-X (diamonds), IBIS/ISGRI (squares) and SPI (circles). The solid line represents the best fit model (BB+PL) to the data. Dashed lines shows the black-body (curved) and power-law models separately.

duration in the γ–ray band) has been carried out for several of the 21 GRBs detected by JEM-X. A rapid decline in the X-ray light curve is expected after the prompt emission, based on the canonical X-ray afterglow behaviour [21].

In the case of GRB 041219A, X-ray emission is detected at the 3.5σ level, beginning at 609 s after the trigger time, for an integration time of 250 s. A power-law model gives the best fit to the spectrum in this interval, with α = -2.2$\pm$0.7 and a flux of 2.9×10^{-10} ergs cm^{-2} s^{-1} in the 3-35 keV energy range. Most of the detected emission comes from the soft band (3-10 keV), with 20% of the measured flux detected in the 10-35 keV band.

Post-burst X-ray emission is also detected in the X-ray rich burst GRB 081003A which has a T_{90}= 22 s. From T_0+22 s to T_0+70 s the X-ray emission decays as a power-law of slope -0.98$\pm$0.05 (Fig. 3). Thereafter the decay slope steepens to a slope of -3.88$\pm$0.11 until T_0+250 s. These results

show the first detection of an X-ray afterglow by *INTEGRAL*.

Later observations (T_0+10^4 s) by *Swift* indicate that the X-ray light curve must flatten out sometime after T_0+250 s. A lower limit on the slope of -0.80±0.14 is derived, assuming the flattening starts at T_0+250 s. Further analysis of the JEM-X data is ongoing.

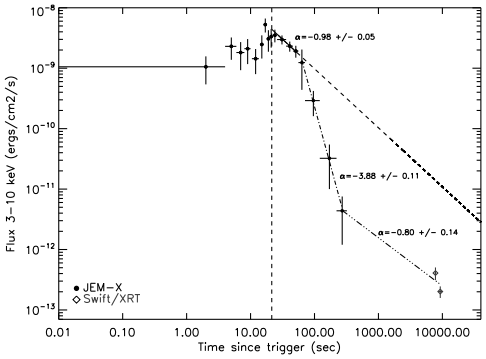

Figure 3: The JEM-X light curve of GRB 081003A in the 3-10 keV band. The vertical dashed line marks the end of the T_{90} measured in the 20-200 keV energy range. The later Swift/XRT data at $\sim 10^4$ s are also shown (grey diamonds).

Acknowledgements

This study is based on observations with *INTEGRAL*, an ESA project with instruments and science data centre funded by ESA member states (especially the PI countries: Denmark, France, Germany, Italy, Switzerland, Spain), Poland and with the participation of Russia and the USA. AMC and LH acknowledge financial support from Science Foundation Ireland grant 09/RFP/AST/2400.

References

[1] Winkler, C.; Courvoisier, G.; Di Cocco, G. et al. 2003, A&A, 411, L1

[2] Ubertini, P.; Lebrun F.; Di Cocco, G. et al. 2003, A&A, 411, L131

[3] Mereghetti, S.; Götz, D.; Borkowski, J. et al. 2003, A&A, 411, L291

[4] Foley, S.; McGlynn, S.; Hanlon, L. et al. 2008 A&A 484, 143

[5] Lund, N.; Budtz-Jorgensen, C.; Westergaard, N. J. et al. 2003, A&A, 411, L223

[6] Vedrenne, G.; Roques, J. P.; Schönfelder, V. et al. 2003, A&A, 411, L63

[7] Piran,T. 2004, Reviews of Modern Physics, Vol. 76, No. 4, pp. 1143-1210

[8] Preece, R. D.; Briggs, M. S.; Mallozzi, R. S. et al. 1998, ApJL, 506, L23

[9] Preece, R. D.; Briggs, M. S.; Pendleton, G. N. et al. 1996, ApJ, 473, 310

[10] Preece, R. D.; Briggs, M. S.; Mallozzi, R. S. et al. 2000, ApJS, 126, 19

[11] Pe'er, A., Ryde, F.; Wijers, R.A.M.J., et al. 2007, ApJ, 664, L1

[12] McBreen, S.; Hanlon, L.; McGlynn, S. et al. 2006, A&A, 455, 433

[13] Ryde, F. 2005, ApJ, 625, pp. L95-L98

[14] Larsson, J.; Ryde, F.; Lundman, C. et al. 2011, MNRAS, 414, 2642

[15] Ackermann, M., et al. 2010, ApJ, 716, 1178

[16] Evans, P. A.; Willingale, R.; Osborne, J. P. et al. 2010, A&A, 519, A102

[17] Evans, P. A.; Osborne, J. P.; Willingale, R. and O'Brien, P. T. 2011, AIP Conference Proceedings, 1358, pp. 117-120

[18] Sari, R. and Piran, T., 1999, ApJ, 520, 641

[19] Martin-Carrillo, A.; Topinka, M.; Hanlon, L. et al. 2011, PoS 8th INTEGRAL Workshop

[20] Gotz, D.; Mereghetti, S.; Paizis, A. et al. 2008, GCN 8377

[21] Zhang, B.; Fan, Y. Z.; Dyks, J. et al. 2006, ApJ, 642, 354